Available online at www.sciencedirect.com
ScienceDirect
Journal of Power Sources 165 (2007) 922–927
JOURNAL OF POWER SOURCES
www.elsevier.com/locate/jpowsour

Short communication

High temperature carbon–carbon supercapacitor using ionic liquid as electrolyte

A. Balducci [a], R. Dugas [a], P.L. Taberna [a], P. Simon [a,*], D. Plée [b], M. Mastragostino [c], S. Passerini [d]

[a] *Université Paul Sabatier, CIRIMAT, UMR CNRS 5085, 118 Route de Narbonne, 31062 Toulouse Cedex, France*
[b] *ARKEMA, GRL, RN 117, 64170 Lacq, France*
[c] *Università di Bologna, Dipartimento di Scienza dei Metalli, Elettrochimica e Tecniche Chimiche, Sede Amministrativa, via San Donato 15, 40127 Bologna, Italy*
[d] *ENEA (Italian National Agency for New Technologies, Energy and Environment), IDROCOMB, Casaccia Research Center, Via Anguillarese 301, 00060 Rome, Italy*

Received 4 August 2006; received in revised form 7 November 2006; accepted 18 December 2006
Available online 3 January 2007

Abstract

This paper presents results about the electrochemical and cycling characterizations of a supercapacitor cell using a microporous activated carbon as the active material and *N*-butyl-*N*-methylpyrrolidinium bis(trifluoromethanesulfonyl)imide ($PYR_{14}TFSI$) ionic liquid as the electrolyte. The microporous activated carbon exhibited a specific capacitance of $60\,F\,g^{-1}$ measured from the three-electrode cyclic voltammetry experiments at $20\,mV\,s^{-1}$ scan rate, with a maximum operating potential range of 4.5 V at 60 °C. A coin cell assembled with this microporous activated carbon and $PYR_{14}TFSI$ as the electrolyte was cycled for 40,000 cycles without any change of cell resistance ($9\,\Omega\,cm^2$), at a voltage up to 3.5 V at 60 °C, demonstrating a high cycling stability as well as a high stable specific capacitance in this ionic liquid electrolyte. These high performances make now this type of supercapacitor suitable for high temperature applications (≥60 °C).

Keywords: Supercapacitor; Ionic liquids; Activated carbon; Microporous carbon

1. Introduction

Supercapacitors are now widely used in power electronics for back-up memories and peak power saving, and today one of the most promising application is their use in transportation field, particularly in hybrid electric vehicle (HEV) [1–6]. In HEV, supercapacitors can be coupled with fuel cells or batteries, to deliver the high power needed during acceleration as well as to recover the energy during braking. In such architectures, operating temperature of 60 °C and more are currently met and this is particularly accurate when these devices are associated with fuel cells.

In the literature, three different types of supercapacitors are commonly described depending on the different active materials used: activated carbon [7,8], metal-oxide [9,10] and electronically conducting polymers [11,12]. In the last few years a new type of supercapacitors has appeared: the hybrid systems, where faradaic and carbon electrodes are associated in order to increase the specific energy [13–15]. Activated carbon-based supercapacitors are the most developed technology because of their low cost, large capacitance and long cycling stability. In these devices the charge storage is electrostatic and the electrolyte ions are reversibly adsorbed in the electrochemical double-layer of the porous carbon electrode structure [16]. The most recent activated carbon supercapacitors on the market use electrolyte solutions based on aprotic solvents, typically acetonitrile (ACN) or carbonate-based solvents (propylene carbonate, ethylene carbonate, etc.) and operate at room temperature (RT) with cell voltage of 2.3–2.5 V. However, for the operating conditions required in HEV applications, these commercial devices are not the best that could be designed to operate at these temperatures because (i) the electrochemical stability window of organic solvents decreases with increasing temperatures [17,18] and (ii) the increase of the maximum cell voltage significantly reduces the cycle-life. Moreover, the high vapour pressure of ACN-based electrolytes requires a careful and too expensive thermal control.

* Corresponding author. Tel.: +33 5 61 55 68 02; fax: +33 5 61 55 61 63.
E-mail address: simon@chimie.ups-tlse.fr (P. Simon).

0378-7753/$ – see front matter © 2007 Elsevier B.V. All rights reserved.
doi:10.1016/j.jpowsour.2006.12.048

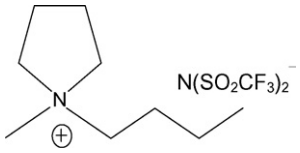

Scheme 1. *N*-Butyl-*N*-methylpyrrolidinium bis(trifluoromethanesulfonyl) imide ($PYR_{14}TFSI$).

Ionic liquids (ILs) are room temperature molten salts, they are entirely composed of cations and anions, the nature of which influences the chemical/electrochemical and physical properties. Particularly, the cation limits the negative potential window while the anion affects the positive potential window as well as the melting point, which in turn affects the working temperature range for high conductivity. ILs typically show a very low vapour pressure, high thermal stability, wide electrochemical windows and good conductivity at temperatures ($\geq$60 °C) required for the HEV supercapacitors application; for these reasons, ILs are very promising candidates to be used as electrolytes in supercapacitors.

Recently, the use of ILs as electrolytes in supercapacitors has been investigated both in double layer activated carbon supercapacitors (DLCSs) and in hybrid polymer supercapacitors [19–27] and the results of these studies are very promising. In fact, the use of ILs as electrolytes in supercapacitors instead of aprotic organic solvents allows the increase of their maximum cell voltage and consequently the improvement of their maximum specific energy, when operating in the temperature range required for HEV applications. The main drawback seems to be the lower specific capacitance values exhibited by the active materials in ILs as compared to ACN-based organic solvents. However, it is important to note that the most part of electrode materials tested in ILs were designed for an use in organic electrolytes. To optimize the performance of the electrochemical systems in ILs, studies are now focused on the selection of materials with higher affinity for ILs.

In this paper, we report and discuss the results of voltammetric study of a new activated carbon (AC) in *N*-butyl-*N*-methylpyrrolidinium bis(trifluoromethanesulfonyl)imide ($PYR_{14}TFSI$, Scheme 1) IL at 60 °C and the results of cycling tests over more than 40,000 cycles for a DLC assembled in coin cell configuration, operating at 60 °C. The $PYR_{14}TFSI$ IL was selected for its electrochemical properties [28,29], its hydrophobic nature, its high level of purity such as that required for long cycle-life, high-voltage supercapacitors.

2. Experimental

The IL $PYR_{14}TFSI$ was prepared as previously described in [29]; the electrolyte water content was less than 10 ppm and it was stored and handled in dry box (Mbraun, UNILAB, H_2O and O_2 <1 ppm).

The composite carbon electrodes were prepared by mixing 95% (w/w) of AC (CECA Acticarbone AB, from CECA company) with 5% (w/w) polytetrafluoroethylene binder (PTFE, Du Pont). The mixture of 95% activated carbon and 5% PTFE will be referred as "active material" in this paper. The active material film thickness was about 300 μm.

Table 1
Ionic conductivity, ionic radius and electrochemical voltage window for the PYRTFSI ionic liquid

	$PYR_{14}TFSI$	PC-LiTFSI
Conductivity at 60 °C (mS cm^{-1})	6.0	9.8
Ionic radius		
Cation (nm)	1.1	0.06
Anion (nm)	0.7	0.35
Stability window (V)	5	3.5

The electrochemical study of CECA Acticarbone AB in $PYR_{14}TFSI$ IL at 60 °C was first achieved using a three-electrode cell assembled in a dry box with working and counter electrodes laminated on Al/C grid (LAMART) and an Ag quasi-reference electrode (ca. +300 mV versus saturated calomel electrode). The working electrode displayed a mass loading of 10 mg cm^{-2}, in order to smooth the voltage shift of the counter electrode, its active mass weight was more than four times higher than one of the working electrode and both displayed a geometric area of 0.25 cm^2. Voltammetric measurements have been performed with an EG&G 263A potentiostat/galvanostat.

For long span life cycling, a standard 2016 coin cell was assembled in a dry box with two carbon composite films laminated on Al current collector foil treated with a chemical etching and a sol–gel deposit [30]. The geometric area of electrodes was 1.13 cm^2 with single electrode mass loading of 19.5 mg cm^{-2}. The separator used was from DURIEUX (no. 28, glass fiber, 350 μm thick) and a 350 μm thick aluminium spacer was used to ensure the pressure inside the coin cell. Galvanostatic cycling measurements were performed using a BT2000 Arbin cycler.

Electrochemical impedance spectroscopy measurements were achieved with an EG&G 6310, between 50 kHz and 10 mHz, at bias voltages of 0 and 3 V, after the first 3000 galvanostatic cycles.

3. Results and discussion

3.1. Preliminary study

Prior to the use of the $PYR_{14}TFSI$ electrolyte in supercapacitors, electrochemical and chemical characterizations have been carried out in order to evaluate the thermal stability, the conductivity and the electrochemical stability window of this IL at 60 °C. These characterizations [24,25] showed that $PYR_{14}TFSI$ was an hydrophobic IL with a very good thermal stability (up to 350 °C), a conductivity and a viscosity of, respectively, 6 mS cm^{-1} and 0.15 Pa s, both at 60 °C, that is comparable to that of many conventional lithium batteries and supercapacitors organic solvents. The maximum stability window is about 6 V that is large enough to allow high operating voltage. Some characteristics are reported in Table 1; and additional parameters have been fully reported in our previous paper [24,25].

Table 2
Physical properties of the CECA "Acticarbone AB" activated carbon

BET surface ($m^2\ g^{-1}$)	1428
Microporous volume ($cm^3\ g^{-1}$), <2 nm	0.596
Mesoporous volume ($cm^3\ g^{-1}$), 2–50 nm	0.03
Macroporous volume ($cm^3\ g^{-1}$), >50 nm	0.141
Resistivity (Ω cm)	0.82
Fe content (ppm)	100

From these previous results, it appeared that $PYR_{14}TFSI$ could be a good candidate to the substitution of the aprotic organic solvents as electrolytes in supercapacitors. Still in the same previous study [24,25], the specific capacitance of the AC electrode, was found to be 50% lower than that displayed by the same electrode in conventional organic electrolytes.

It is known that the wettability of carbon by the electrolytes depends on its pore size distribution and on the chemical groups present on its surface. Recently, several types of activated carbon have been tested in different ILs [24,30,32,33] and the most part of these carbons are tailored in the mesoporous region. In a recent paper, it was demonstrated that microporous pores contribute to the charge storage in porous carbons, leading to high energy density materials [34]. In order to find an AC able to display a high value of volumetric capacitance and a large cycle stability in $PYR_{14}TFSI$, we selected a new type of AC, namely CECA Acticarbone AB, from the CECA company whose characteristics are given in Table 2. As it can be seen in this table, the CECA Acticarbone AB has a porosity tailored in the microporous region, i.e. with pore radius between 1 and 2 nm.

3.2. Three-electrode cyclic voltammetry experiments

The performances of carbon CECA Acticarbone AB were evaluated at 60 °C in $PYR_{14}TFSI$, in terms of negative ($V_{min,-}$) and positive ($V_{max,+}$) potential limits versus the reference electrode; the potentials limits were defined to maintain the charge–discharge coulombic efficiency (η, %) higher than 95%. Fig. 1 shows the cyclic voltammetry (CV) of an electrode (95 wt.% of activated carbon–5% PTFE) at 60 °C in the $PYR_{14}TFSI$ ionic liquid, expressed in terms of specific capacitance in farad per gram of active material, C_{am}, versus the potential. The scan rate is 20 mV s^{-1}. C_{am} is obtained by dividing the current density by the scan rate and the mass of the electrode active material, w_{am}. The minimum potential is −2.7 V versus Ag, and the maximum one is $V_{max,+}$ = +1.8 V versus Ag^+/Ag reference electrode; the CV curve does not exhibit any faradaic peaks. The maximum cell voltage of 4.5 V is a high operating potential range for an AC in ILs. The inset in Fig. 1 presents the change of the activated carbon specific capacitance with the scan rate. It is calculated from the integral of the CV curves.

A specific capacitance of 90 F g^{-1} is obtained at 5 mV s^{-1}. This value is in the same range of the ones achieved with standard activated carbons in aprotic liquid electrolyte. When the scan rate is increased, the specific capacitance is decreased down to 60 F g^{-1}: this was an expected behavior since the ionic liquid

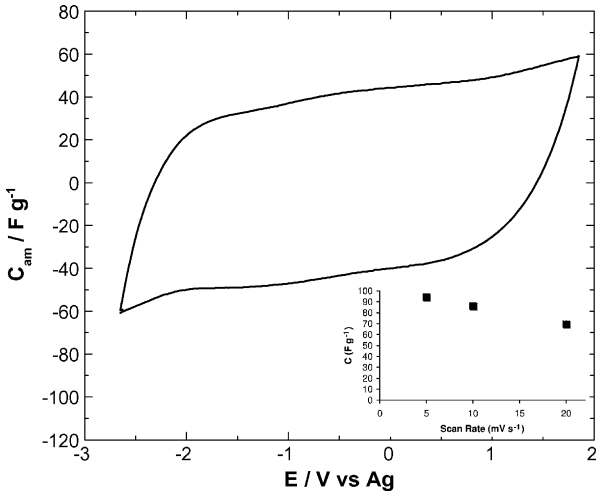

Fig. 1. Specific capacitance values of CECA "Acticarbone AB" electrode in $PYR_{14}TFSI$ electrolyte at 60 °C, obtained from CV at 20 mV s^{-1} by dividing specific current by the scan rate. Inset: capacitance change with the potential scanning rate deduced from CV experiments.

conductivity is lower as compared to ACN or carbonates-based electrolytes.

However, high value of $\Delta V_{max} = V_{max+} - V_{min-}$ will allow to improve the storage capability according to the following equation:

$$E_{max} = \tfrac{1}{2} C_{tcm}\, \Delta V_{max}^2 \quad (1)$$

while the power loss due to the increase of the series resistance will be buffered by the increase of the maximum cell voltage according to the following equation:

$$P_{max} = \frac{V_{max}^2}{4\,ESR\, w_{tam}} \quad (2)$$

where in Eqs. (1) and (2) C_{tcm} is the total cell capacitance per weight unit of the active material film (including binder and carbon), ESR the equivalent series resistance measured at 1 kHz and w_{tam} is the total weight of the two electrodes active materials per geometric area.

This microporous activated carbon seems to be a very promising candidate as active material for carbon–carbon supercapacitor electrodes using $PYR_{14}TFSI$ as electrolyte.

3.3. Coin cell assembly and electrochemical tests

On the basis of the potential limits previously defined, a DLC supercapacitor coin cell activated carbon/$PYR_{14}TFSI$/activated carbon was assembled and tested at 60 °C. The total mass of composite material, w_{tcm}, was 39 mg cm^{-2} (19.5 mg cm^2 on each electrode).

The supercapacitor was first tested by carrying out galvanostatic charge–discharge cycles at different current densities (10, 50 and 100 mA cm^{-2}) up to 28,000 cycles between 0 and 2.75 V. This value of ΔV_{max} = 2.75 V is clearly lower as compared to the maximum value of 4.5 V previously measured for the activated carbon in $PYR_{14}TFSI$ at 60 °C. However, it is already high when

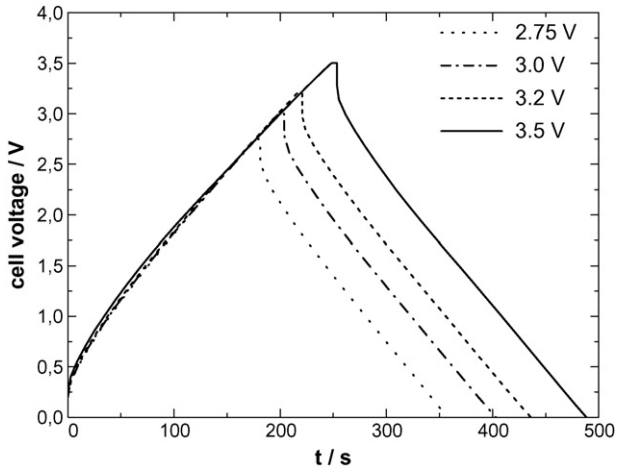

Fig. 2. Voltage profiles of the CECA "Acticarbone AB"/$PYR_{14}TFSI$/CECA "Acticarbone AB" supercapacitor at 10 mA cm^{-2} and 60 °C for different cell cut-off.

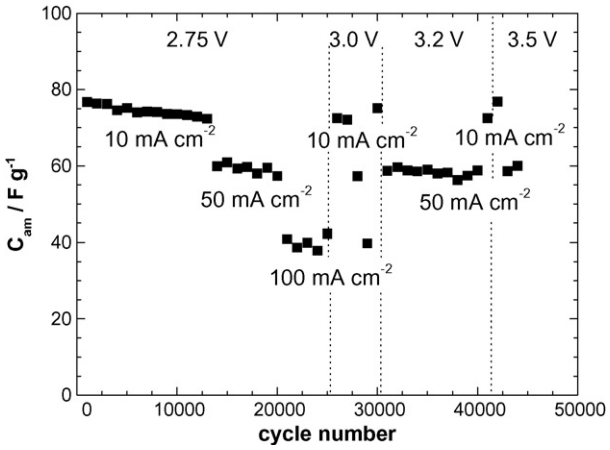

Fig. 4. Change of the specific capacitance of active material vs. cycles number for the CECA "Acticarbone AB"/$PYR_{14}TFSI$/CECA "Acticarbone AB" supercapacitor from galvanostatic cycles at 10, 50, and 100 mA cm^{-2} for different cell cut-off at 60 °C.

compared to the values of ΔV_{max} normally displayed by DLCs using liquid organic electrolytes.

After these cycles, ΔV_{max} was successively increased from 3.0 V, up to 3.5 V and several thousands of galvanostatic cycles were carried out for each V_{max}. Fig. 2 shows the voltage profiles at a current density of 10 mA cm^{-2} for the four different potential ranges studied. For each ΔV_{max}, the voltage profile of the activated carbon in $PYR_{14}TFSI$ at 60 °C exhibits a linear shape demonstrating the absence of faradaic reaction in this potential window, like in the classic organic electrolytes [30,35]. However, with respect to the organic aprotic electrolytes, especially the ACN-based ones, ESR is 10-fold higher because of the lower conductivity of $PYR_{14}TFSI$ at 60 °C. The influence of this low conductivity is also clearly visible in the Nyquist plots reported in Fig. 3 after 3000 cycles, at bias cell voltages of 0 and 3 V. As can be seen, these plots are shifted to higher values of the real part of the impedance and the low frequency straight line is not as vertical as those obtained with acetonitrile-based solvents [30,31]. It has been already demonstrated elsewhere [31] that impedance of the cell is largely dependant of the conductivity of the electrolyte and the viscosity as well. In our case it is emphasized because of the cell configuration. Indeed, a 350 μm thick separator was used in order to avoid short circuits during the sealing process of the coin cells; this, associated with the lower ionic conductivity of the ionic liquids as compared to the classical electrolytes [30,35], limits the power performances of the cell.

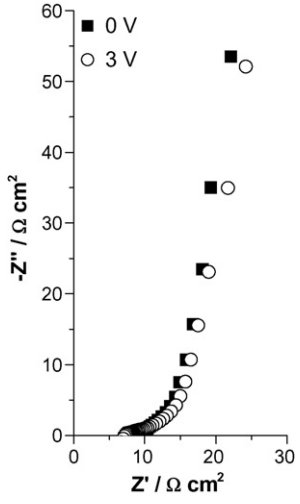

Fig. 3. Nyquist plots of the CECA "Acticarbone AB"/$PYR_{14}TFSI$/CECA "Acticarbone AB" supercapacitor at 60 °C at 0 and 3 V.

In Fig. 4 is reported the change of the specific capacitance C_{am} versus the cycles numbers for different current densities and different ΔV_{max}. The cell capacitance was calculated from the slope of the discharge curve according to the following equation:

$$C = \frac{I}{dV/dt} \quad (3)$$

where C is the capacitance of the cell in farad, I the discharge current in ampere (A) and dV/dt is the slope in volt per second (V s^{-1}).

In a symmetrical system where the active material weight is the same for the two electrodes, the specific capacitance, C_{am}, in farad per gram of active material (F g^{-1}) is related to the capacitance of the cell by:

$$C_{am} = \frac{2C}{m_{am}} \quad (4)$$

where m_{am} is the weight per electrode of active material (g).

It can be seen in Fig. 4, that the value of the specific capacitance calculated at 10 mA cm^{-2} is stable over 40,000 cycles and did not significantly change when ΔV_{max} is increased, thus demonstrating a very high cycling stability for microporous activated carbon in $PYR_{14}TFSI$. In addition, it is important to note that the value of C_{am} was clearly modified during the changes in current densities as it is generally observed [36] but each time that the current density was set back at 10 mA cm^{-2} the C_{am} initial value was recovered.

Fig. 5 reports the change of the equivalent series resistance (ESR, in Ω cm^2) calculated from the ohmic drop, occurring dur-

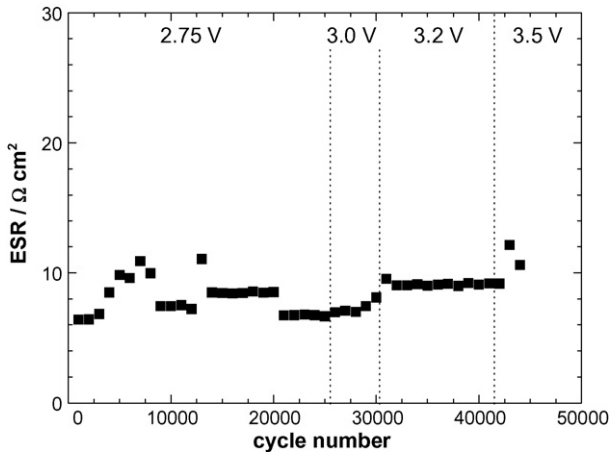

Fig. 5. Change of the ESR value (measured at a frequency of 1 kHz) vs. cycles number of the CECA "Acticarbone AB"/$PYR_{14}TFSI$/CECA "Acticarbone AB" supercapacitor from galvanostatic cycles at 10, 50, and 100 mA cm^{-2} for different cell cut-off at 60 °C.

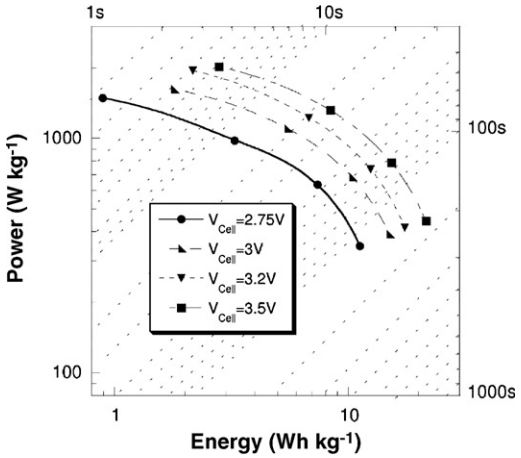

Fig. 6. Ragone plot for the activated carbon/PYRTFSI/activated carbon coin cell; energy and power densities related to active materials mass.

ing the first 1 ms current, at the beginning of the discharge versus the cycling number, for different ΔV_{max} and for different current densities. The ESR value remains lower than 10 Ω cm^2 over the 40,000 cycles whatever the current density. As compared to the value usually reported for DLCs using ACN-based electrolytes [30,35] the ESR is clearly higher (one order of magnitude). However, when compared to others systems using ILs as electrolytes [24–26,21], this value of ESR is lower and more or less constant for an impressive number of cycles. This can also be associated with the use of treated Al current collector previously reported [30].

Fig. 6 sums up in a Ragone plot the performances reached at different cell voltages. This plot reports mean values obtained in galvanostatic charge–discharge experiment taking into account the losses due to ohmic drop. These energy density values are then the real energy (and not the calculated) the cell can deliver. Values as high as 2 kW kg^{-1} and 20 Wh kg^{-1} of active material are reached at a cell voltage of 3.5 V.

Table 3 lists the maximum specific energy (E_{max}) and power (P_{max}), the coulombic efficiency (η, %), the specific capacity delivered per gram of total active material of the two-electrode cell (Q_{tam}) and the capacitance per gram of total active material of the two-electrode cell (C_{tam}), displayed at the last cycles at the current density of 10 mA cm^{-2}. Note that for ΔV_{max} = 3.5 V, the coulombic efficiency was only 95% even at the beginning of the cycling.

Table 3 shows the value of C_{tam} remains constant for the different values of ΔV_{max}, in agreement with the constant value of the slope of the discharge curves presented in Fig. 2. The increase of ΔV_{max} along with the constant discharge plot slopes lead to an increase of the discharge time and consequently to the improvement of Q_{tam} up to 16.8 mAh g^{-1} at 3.5 V. The value of ESR at 10 mA cm^{-2} remains lower than 10 Ω cm^2 in the whole potential range explored. According to Eq. (2), the value of P_{max} globally increases with ΔV_{max}, and at 3.5 V this value is 8.6 kW kg^{-1} of total active material. The value of E_{max}, according to Eq. (1), increases while ΔV_{max} increases; it reaches 31 Wh kg^{-1} of total active material at 3.5 V. However, this high value for an ionic liquid-based supercapacitor was obtained as the coulombic efficiency was decreased down to 95%, which is a low value that cannot guarantee a long cycle-life for the supercapacitor (>100,000 cycles). It will be necessary to evaluate whereas this low value of the coulombic efficiency is due to the high number of cycles previously achieved before the increase at ΔV_{max} = 3.5 V or if this ΔV_{max} is the real voltage limit for a DLC coin cell using this microporous activated carbon in $PYR_{14}TFSI$ at 60 °C.

The performances of the supercapacitor microporous activated carbon/$PYR_{14}TFSI$/microporous activated carbon using CECA Acticarbone are very promising. These good capacitance values (up to 90 F g^{-1} in the $PYR_{14}TFSI$ electrolyte) with this microporous carbon are in good agreement with recent results [34]. Work is in progress to decrease the resistance using specific surface treatments onto the Al foil current collector, in order to

Table 3
Coulombic efficiency values (η, %) of the charge–discharge processes, equivalent series resistance (ESR at 1 kHz), specific capacitance value per gram of total active material (on the two electrodes) (C_{tam}), specific capacity value per gram of total active material (Q_{tam}), maximum specific energy (E_{max}) and maximum specific power (P_{max}) for the CECA "Acticarbone AB"/$PYR_{14}TFSI$/CECA "Acticarbone AB" supercapacitor obtained during cycling at 10 mA cm^{-2} for different cut-off potential, at 60 °C

Cut-off potential (ΔV_{max} in V)	η (%)	ESR (Ω cm^2)	C_{tam} (F g^{-1})	Q_{tam} (mAh g^{-1})	E_{max} (Wh kg^{-1})	P_{max} (kW kg^{-1})
0–2.75	100	9.9	18.2	12.3	19.2	4.9
0–3.00	100	8.1	18.8	14.2	23.5	7.1
0–3.20	100	9.4	18.9	15.4	26.9	7.0
0–3.50	95	9.2	18.2	16.8	31.0	8.6

increase the power delivered by these system, to make them fully attractive for power applications at high temperature for HEV applications.

4. Conclusion

Microporous activated carbon from CECA company (Acticarbone AB) shows a very good value of specific capacitance in $PYR_{14}TFSI$ as well as a remarkable cycling stability. To our knowledge, the activated carbon/$PYR_{14}TFSI$/activated carbon is the first example of DLCS using an IL as electrolyte working with ΔV_{max} up to 3.5 V and at 60 °C, stable for several thousands galvanostatic cycles. After 40,000 cycles, at $V_{max} = 3.5$ V, the supercapacitor maximum specific energy and power are $E_{max} = 31\ Wh\ kg^{-1}$ and $P_{max} = 8.6\ kW\ kg^{-1}$, respectively. This value of E_{max} is higher than the one normally achieved with DLCs in ACN-based electrolytes, but the value of P_{max} is lower. However, this power decrease due to the lower ionic conductivity of the Ionic Liquids as compared to aprotic electrolytes, is buffered by the increase of the working voltage of the cell, up to 3.5 V.

Acknowledgements

The authors wish to thank the Italian–French University for providing a PhD Grant to Andrea Balducci as part of the Vinci Project 2003, involving Paul Sabatier University of Toulouse (France) and Bologna University (Italy). Romain Dugas was funded by the European Commission STREP "ILHYPOS" project #51307, 6th PCRD.

References

[1] R. Kotz, M. Carlen, Electrochim. Acta 45 (2000) 2483.
[2] A. Burke, J. Power Sources 91 (2000) 37.
[3] M. Mastragostino, C. Arbizzani, F. Soavi, in: W.A. Van Schalkwijk, B. Scrosati (Eds.), Advances in Lithium-ion Batteries, Kluwer Academic Publishers/Plenum Press, New York, 2002 (Chapter 16).
[4] R.J. Brodd, K.R. Bullock, R.A. Leising, R.L. Middaugh, J.R. Miller, E. Takeuchi, J. Electrochem. Soc. 151 (2004) K1.
[5] A. Rufer, IEEE Trans. Power Deliv. 19 (2004) 629.
[6] P. Rodatz, G. Paganelli, A. Sciarretta, L. Guzzella, Control. Eng. Pract. 13 (2005) 41.
[7] D. Lazano-Castello, D. Carzorla-Amoros, A. Linares-Solano, S. Shiraishi, H. Kurihara, A. Oya, Carbon 41 (2003) 1765.
[8] J. Gamby, P.L. Taberna, P. Simon, J.F. Fauvarque, M. Chesneau, J. Power Sources 101 (2001) 109.
[9] Q.L. Fang, D.A. Evans, S.L. Roberson, J.P. Zheng, J. Electrochem. Soc. 148 (2001) A833.
[10] J. Jiang, A. Kucernak, Electrochim. Acta 47 (2002) 2381.
[11] M. Mastragostino, C. Arbizzani, F. Soavi, Solid State Ionics 148 (2002) 493.
[12] W.C. Chen, T.C. Wen, H. Teng, Electrochim. Acta 48 (2003) 641.
[13] A. Laforgue, P. Simon, J.F. Fauvarque, M. Mastragostino, F. Soavi, J.F. Sarrau, P. Lailler, M. Conte, E. Rossi, S. Saguatti, J. Electrochem. Soc. 150 (2003) A645.
[14] A. Du Pasquier, I. Plitz, J. Gural, S. Menocal, G. Amatucci, J. Power Sources 113 (2003) A645.
[15] A. Burke, Proceedings of the Third International Advanced Automotive Battery Conference, Nice, France, 10 June, 2003.
[16] B.E. Conway, Electrochemical Capacitor, Scientific Fundamentals and Technological Application, Plenum Press, New York, 1999, p. 105.
[17] M. Ue, K. Ida, S. Mori, J. Electrochem. Soc. 141 (1994) 2989.
[18] R. Koetz, M. Hahn, O. Barbieri, R. Gallay, Proceedings of the 55th Annual Meeting of the International Society of Electrochemistry, 19–26 September, Thessaloniki, Greece, 2004 (Abst. S9FP166).
[19] A. Lewandowski, A. Swiderska, Solid State Ionics 161 (2003) 243.
[20] M. Ue, M. Takeda, A. Toriumi, A. Kominato, R. Hagiwara, Y. Ito, J. Electrochem. Soc. 150 (2003) A499.
[21] A. Lewandowski, M. Galinski, J. Phys. Chem. Solids 65 (2004) 281.
[22] J.D. Stenger-Smith, C.K. Webber, N. Anderson, A.P. Chafin, K. Zong, J.R. Reynolds, J. Electrochem. Soc. 149 (2002) A973.
[23] E. Nandin, H.A. Ho, S. Branchaud, L. Breau, D. Belanger, J. Phys. Chem. B 106 (2002) 10585.
[24] A. Balducci, W.A. Henderson, M. Mastragostino, S. Passerini, P. Simon, F. Soavi, Electrochim. Acta 50 (2005) 2233.
[25] A. Balducci, M. Mastragostino, F. Soavi, Appl. Phys. A 82 (2005) 627–632.
[26] A. Balducci, U. Bardi, S. Caporali, M. Mastragostino, F. Soavi, Electrochem. Commun. 6 (2004) 566.
[27] B. Xu, F. Wu, R. Chen, G. Cao, S. Chen, G. Wang, Y. Yang, J. Power Sources 158 (2006) 773.
[28] D.R. MacFarlane, P. Maekin, J. Sua, N. Amini, M. Forsyth, J. Phys. Chem. B 103 (2003) 4164.
[29] W.A. Henderson, S. Passerini, Chem. Mater. 16 (2004) 2881.
[30] C. Portet, P.L. Taberna, P. Simon, C. Laberty-Robert, Electrochim. Acta 49 (2004) 905.
[31] P.L. Taberna, P. Simon, J.F. Fauvarque, J. Electrochem. Soc. 150 (3) (2003) A292–A300.
[32] J.N. Barisci, G.G. Wallace, D.R. MacFarlane, R.H. Baughman, Electrochem. Commun. 6 (2004) 22.
[33] T. Sato, G. Masuda, K. Takagi, Electrochim. Acta 49 (2004) 3603.
[34] J. Chmiola, G. Yushin, Y. Gogotsi, C. Portet, P. Simonand, P.L. Taberna, Science 313 (2006) 1760–1763. Published online 17 August 2006; 10.112/science/1132195.
[35] C. Portet, P.L. Taberna, P. Simon, E. Flahaut, C. Laberty-Robert, Electrochim. Acta 50 (2005) 4174.
[36] C. Portet, P.L. Taberna, P. Simon, E. Flahaut, J. Power Sources 139 (2005) 371.